Göde, F., Çelik, A. (2024). The Structural and Optical Properties of Polycrystalline Copper Oxide Thin Films Synthesized Using the SILAR Technique. *The Black Sea Journal of Sciences*, 14(4), 2216-2226.

The Black Sea Journal of Sciences, 14(4), 2216-2226, 2024. DOI: 10.31466/kfbd.1543126

KFBD

Karadeniz Fen Bilimleri Dergisi
The Black Sea Journal of Sciences
ISSN (Online): 2564-7377 https://dergipark.org.tr/tr/pub/kfbd

Araştırma Makalesi / Research Article

The Structural and Optical Properties of Polycrystalline Copper Oxide Thin Films Synthesized Using the SILAR Technique

Fatma GÖDE[1], Ali ÇELİK[2*]

Abstract

In this study, polycrystalline copper oxide (CuO) thin films with the presence of various pH levels were fabricated using the successive ion layer adsorption and reaction (SILAR) method. The impact of pH on the structural and optical properties of the produced films was examined. The present films were characterized by X-ray diffraction (XRD) and UV-vis absorption spectroscopy measurements. The XRD result showed that all films had a polycrystalline nature with a monoclinic CuO crystal phase. Direct optical band gap energies of the films, determined using the Tauc equation, ranged from 1.49 eV to 2.89 eV. The optical parameters such as refractive index (n), extinction coefficient (k), real (ε_1), and imaginary (ε_2) parts of the dielectric constant were derived from the absorbance and transmittance spectra of the produced films. CuO thin film n values ranged from 3.10 to 11.14, while k values varied from 0.79 to 1.70. Likewise, the values of ε_1 and ε_2 for CuO thin films ranged from 8.96 to 121.15 and 4.89 to 37.90, respectively.

Keywords: Copper Oxide, Thin films, XRD, Band gap energy, Optical parameters.

SILAR Tekniği Kullanılarak Sentezlenen Polikristal Copper Oxide İnce Filmlerin Yapısal ve Optiksel Özellikleri

Öz

Bu çalışmada farklı pH değerlerinde polikristal bakır oksit (CuO) yarı iletken ince filmleri ardışık iyon tabakası adsorpsiyonu ve reaksiyon (SILAR) tekniği kullanılarak elde edilmiştir. Üretilen ince filmlerin yapısal ve optik karakteristikleri üzerinde pH'ın etkisi incelenmiştir. Filmler, X-ışınları kırınımı (XRD) ve Uv-vis spektroskopisi ölçümleri ile karakterize edilmişlerdir. XRD bulguları, elde edilen tüm filmlerin kristal yapıda monoklinik CuO fazına sahip olduğunu göstermiştir. Tauc bağıntısı kullanılarak, filmlerin direkt optik bant aralığı enerjilerinin 1.49 eV ile 2.89 eV arasında değiştiği belirlenmiştir. Optik parametreler; kırılma indisi (n), sönüm katsayısı (k), dielektrik sabitinin real (ε_1), ve sanal (ε_2) kısımları soğurma ve geçirgenlik ölçümleri kullanılarak hesaplanmıştır. CuO ince filmin n değerleri 3.10 ile 11.14 arasında değişirken k değerleri 0.79 ile 1.70 arasında değişmiştir. Benzer şekilde CuO ince filmleri için ε_1, ve ε_2 değerleri sırasıyla 8.96 ile 121.15 ve 4.89 ile 37.90 arasında değişmiştir.

Anahtar Kelimeler: Bakır oksit , İnce filmler, XRD, Bant aralığı enerjisi, Optik parametreler.

[1,2]Burdur Mehmet Akif Ersoy University, Department of Physics, Burdur, Türkiye, ftmgode@gmail.com alicelik@mehmetakif.edu.tr

[*]Sorumlu Yazar/Corresponding Author
Geliş/Received: 03.09.2024 **Kabul/Accepted:** 02.12.2024 **Yayın/Published:** 15.12.2024

1. Introduction

Recently, copper oxide (CuO) has attracted significant interest as a p-type metal oxide due to its wide direct band gap, ranging from 1.29 eV (Alami et al., 2014) to 2.50 eV (Abdelmoneim et al., 2024), as well as its non-toxicity, transparency, conductive nature, and excellent chemical stability. These attributes render it versatile for diverse technological applications, including cool thermal energy storage systems (Srinivasan & Ponnusamy, 2024), photoelectrochemical water-splitting (Abdelmoneim et al., 2024), sensors (Gnanasekar et al., 2021), solar cells (Kumar et al., 2024), organic light-emitting diodes (Kandulna et al., 2023), heterojunction bipolar transistors (Yousefizad et al., 2023), catalytic activity (Arulkumar & Thanikaikarasan, 2024), photodetectors (Yahya Salih et al., 2024), photodegradation (Hassan et al., 2024), and supercapacitors (Narale et al., 2024) .

Various techniques are employed for the production of CuO thin films, such as the chemical bath deposition technique (CBD) (Sultana et al., 2017), spray pyrolysis (Babu et al., 2020), sol-gel (Anitha et al., 2024), vacuum evaporation (Djebian et al., 2020), reactive DC magnetron sputtering (Sahu et al., 2020) and the successive ion layer adsorption and reaction (SILAR) technique (Mageshwari & Sathyamoorthy, 2013). Among these techniques, SILAR stands out for its simplicity and cost-effectiveness. It allows for the facile coating of substrates at ambient or lower temperatures by immersing them sequentially in cationic and anionic precursor solutions, followed by rinsing with ultra-pure water after each immersion cycle to achieve deposition. The deposition cycles in SILAR can be adjusted to control film thickness and deposition rate, offering flexibility in tailoring film properties.

This study focuses on fabricating CuO thin films on glass substrates using the SILAR method. To observe the impact of pH variations on the deposited films, the pH values were adjusted within the range of 9.48 to 10.94. The films' crystallinity and structural characteristics were evaluated using X-ray diffraction (XRD), while their optical properties were analyzed using an ultraviolet-visible (UV-Vis) spectrophotometer. Spectral data from UV-Vis measurements provided insights into the films' absorbance and transmittance, enabling the determination of key optical parameters.

2. Materials and Methods

Materials and methodology used in the conducting of the research need to be described in detail in this section. Using the SILAR method, CuO thin films were synthesized onto microscope glass substrates measuring 76 mm × 26 mm × 1 mm at a controlled temperature of 45 °C. Prior to deposition, the substrates underwent a cleaning process that included washing with detergent and boiling in deionized water. Subsequently, they were sequentially cleaned with methanol, acetone, and

deionized water, with each step lasting fifteen minutes to ensure surface purity and preparation for film deposition.

The deposition process involved immersing the cleaned substrate in a 0.1 M copper (II) nitrate trihydrate [Merck mark; Cu(NO3). 3H2O; 241.60 g/mol; >99.5 purity] precursor solution for 25 s, followed by a thorough rinse with deionized water for another 25 s to eliminate any unreacted ions. This SILAR process was repeated 25 times, resulting in the deposition of a thin film of CuO on microscope glass substrates.

In order to investigate the impact of pH on the deposited films, the pH values of the copper solution were adjusted to values of 9.48, 10.08, and 10.94, by adding a diluted 25% ammonium (NH4) solution. At the end of the experiments, three CuO thin films were deposited, each corresponding to a different pH value. Remarkably, as the film thickness increased, there was a noticeable transition in the film color from brown to a darker shade of brown.

The structure and lattice parameters of CuO films were analyzed by a Bruker A8 Advanced X-ray diffractometer (XRD) with Cu Kα (λ = 0.154 nm) radiation. The optical properties of the films were measured using a UV-Vis spectrophotometer (PG-T60) within the wavelength range of 300–1100 nm. The thickness of the films (t) was determined using a precision microbalance and the gravimetric method, applying the formula $(t = m/\rho S)$, where m is the mass of the film, S is its surface area, and ρ is the density of CuO (6.51 g/cm^3). The thicknesses of the prepared films were determined as 1271 nm, 972 nm, and 1713 nm with pH values of 9.48, 10.08, and 10.94, respectively.

3. Findings and Discussion

The crystallinity of the CuO thin films was analyzed using X-ray diffraction analysis and the findings are depicted in Figure 1. The XRD patterns of CuO, exhibited distinct peaks at 2θ values of ~35.789°, and ~39.248°, corresponding to the (1 1 $\bar{1}$) and (2 0 0) lattice planes, respectively. These peaks are characteristic of the monoclinic phase of CuO, consistent with the reference data (JCPDS card No. 98-008-7126; a = 4.6890 Å; b = 3.42.00 Å; c = 5.1300 Å). The presence of these peaks in the XRD spectra confirms the successful formation of CuO thin films on the microscope glass substrates, validating the crystalline structure of the deposited material.

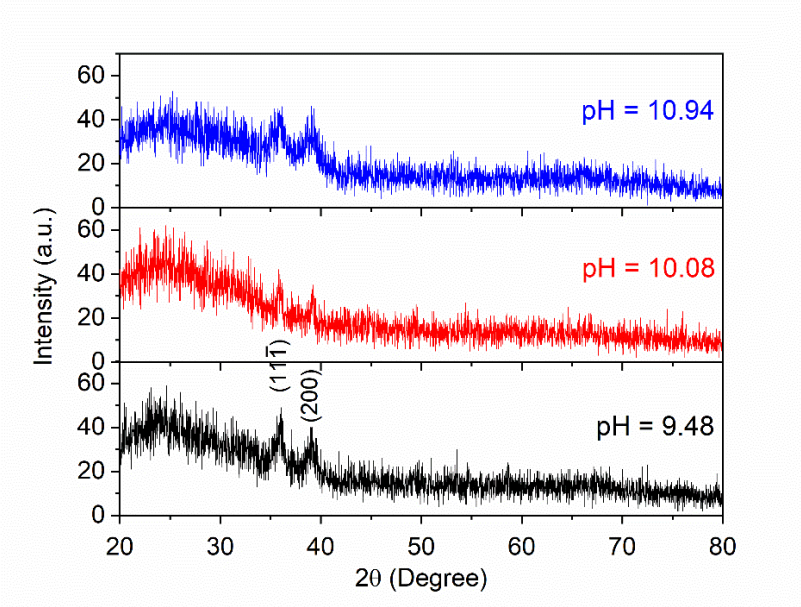

Figure 1. The XRD spectrum of CuO thin films with various pH values.

CuO thin film crystallite sizes were determined using the Scherrer equation (Cullity et. al., 2001):

$$D = \frac{0.9\lambda}{\beta cos\theta} \quad (1)$$

where λ is the wavelength of the light used, β is the full width of the peak at half maximum (FWHM) intensity in radians, and θ is Bragg's angle. The length of the dislocation lines per unit volume of the crystal is known as the dislocation density (δ), which indicates the quantity of defects in the film and is computed using the Equation (2) (Shkir et al., 2019):

$$\delta = \frac{1}{D^2} \quad (2)$$

The Equation (3) was used to calculate the lattice strain (ε) in the CuO films caused by crystal imperfection and distortion (Shkir et al., 2019):

$$\varepsilon = \frac{\beta cos\theta}{4} \quad (3)$$

The calculated crystallite size, dislocation density, and strain values of the films are listed in Table 1. As seen, the highest crystallite sizes were obtained at pH = 10.08 compared with the other pH values. Moreover, it can be said that the small δ and ε values indicate that the films have good

crystallization. As can be seen from Table 1, the lowest δ and ε values were observed as 0.19×10^{10} - 0.17×10^{10} and 1.67×10^{-3} - 1.52×10^{-3}, respectively, for the film obtained at pH = 10.08. Observed *'d'* values of the films were in good agreement with the standard *'d'* values seen in

Table **1**.

Table 1. Observed and standard structural parameters of CuO thin films.

pH	Observed values		Standard values			D (nm)	FWHM (°) = β	$\delta_{avg} \times 10^{10}$ (lines / cm^2)	$\varepsilon_{avg} \times 10^{-3}$	(h k l)
	2θ (º)	d (Å)	2 θ (º)	d (Å)	I (%)					
9.48	36.101	2.4859	35.558	2.5227	75.1	120.9	0.768	0.68	3.19	(1 1 $\bar{1}$)
	39.015	2.3067	38.925	2.3118	22.7	145.8	0.642	0.47	2.64	(2 0 0)
10.08	35.789	2.5069	35.558	2.5227	75.1	229.9	0.403	0.19	1.67	(1 1 $\bar{1}$)
	39.248	2.2936	38.925	2.3118	22.7	252.5	0.371	0.17	1.52	(2 0 0)
10.94	35.421	2.5321	35.558	2.5227	75.1	104.2	0.889	0.92	3.69	(1 1 $\bar{1}$)
	39.340	2.2884	38.925	2.3118	22.7	216.1	0.434	0.21	1.78	(2 0 0)

The direct optical band gap energies and optical parameters of the films were determined through UV–vis absorption and transmission measurements, as depicted in Figure 2 (a) and Figure 2 (b), respectively. To derive these values, the fundamental absorption coefficient (α) was estimated using the following formula (Perkowitz, 1993):

$$T = e^{-\alpha t} \tag{4}$$

where t is the film thickness, and T denotes the transmittance, which is defined as $T = I/I_0$, where I is the intensity of light that passes through the back surface of the film, and I_0 is the incident intensity. This relationship allowed for the precise calculation of the absorption coefficient, which in turn facilitated the determination of the films' optical properties, including their direct band gap energies.

The following formulas were used to determine the reflection (R) (Göde, 2019), and α for CuO thin films based on absorption (A), transmission, and film thickness (Shkir et al., 2016):

$$T = (1 - R)^2 \exp(-A) \tag{5}$$

$$\alpha = 2.303 * A/t \tag{6}$$

The dependence of R and α on wavelength of the films is shown in Figures 2 (c) and (d), respectively. As can be seen, the value of α is on the order of 10^8 (cm^{-1}).

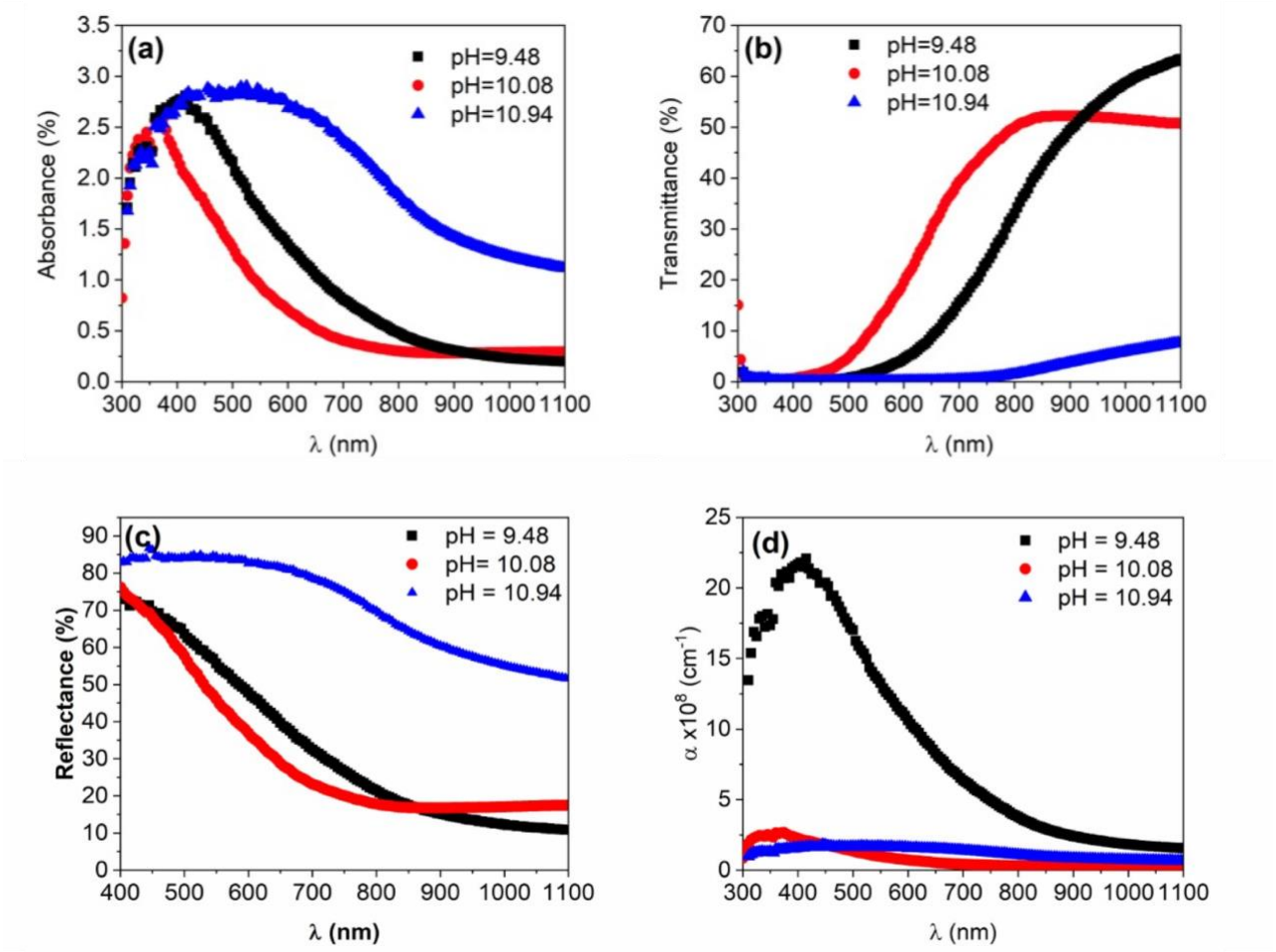

Figure 2. The dependence of **(**a) absorbance spectra, (b) transmittance spectra, (c) reflectance spectra, and (d) absorption coefficient of the CuO thin films on wavelength with varying pH values.

The direct optical band gap energies (E_g) of the films were obtained using the Tauc relation (Pankove, 1975):

$$(\alpha h\nu) = B(h\nu - E_g)^n \quad (7)$$

In the equation above, B is a constant, and $h\nu$ represents the photon energy. For direct transitions, the value of n is ½. By applying this relationship, the optical band gap energies of CuO thin films synthesized at different pH levels of 9.48, 10.08, and 10.98 were found to be 2.18 eV, 2.89 eV, and 1.49 eV, respectively (see Figure 3). Notably, the highest direct band gap energy was 2.89 eV, observed in the film fabricated at a pH of 10.08. These measured optical band gaps are consistent with previously reported values, which range from 1.25 eV to 2.85 eV (Chen et al., 2018; Nitta et al., 2022; Sagadevan et al., 2017). This agreement further validates the accuracy and reliability of the

obtained results, highlighting the significant impact of pH on the optical properties of the CuO thin films.

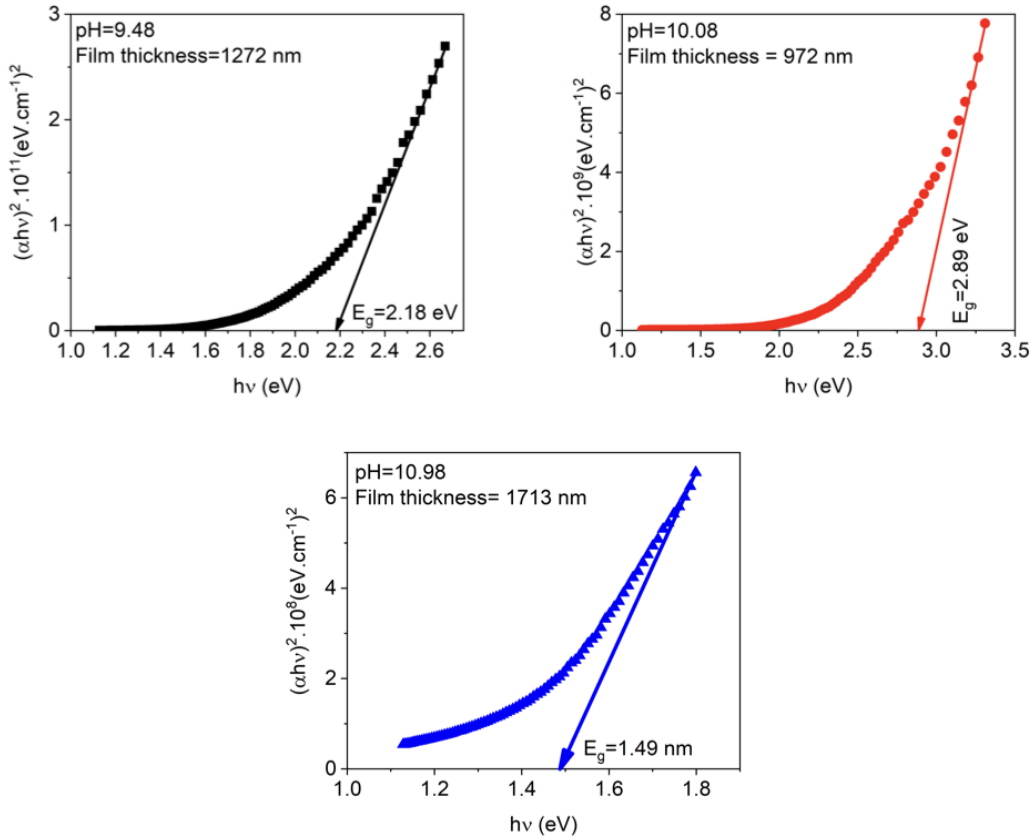

Figure 3. Dependence of $(\boldsymbol{\alpha h\nu})^2$on $(\boldsymbol{h\nu})$ of CuO thin films with varying pH values.

The refractive index (n) and extinction coefficient (k) of CuO thin films are directly related to the absorption coefficient and can be calculated using the following formulas (Gode et al., 2014):

$$k = \frac{\alpha\lambda}{4\pi} \tag{8}$$

$$n = \frac{1+R}{1-R} + \sqrt{\frac{4R}{(1-R)^2} - k^2} \tag{9}$$

The dependence of n and k of the CuO films is indicated in Figure 4(a) and Figure 4(b), respectively. Additionally, their values at a wavelength of 600 nm are summarized in Table 2. At a 600 nm wavelength, as can be seen from this table, the n and k values for CuO thin films ranged from 3.10 to 11.14 and from 0.79 to 1.70, respectively.

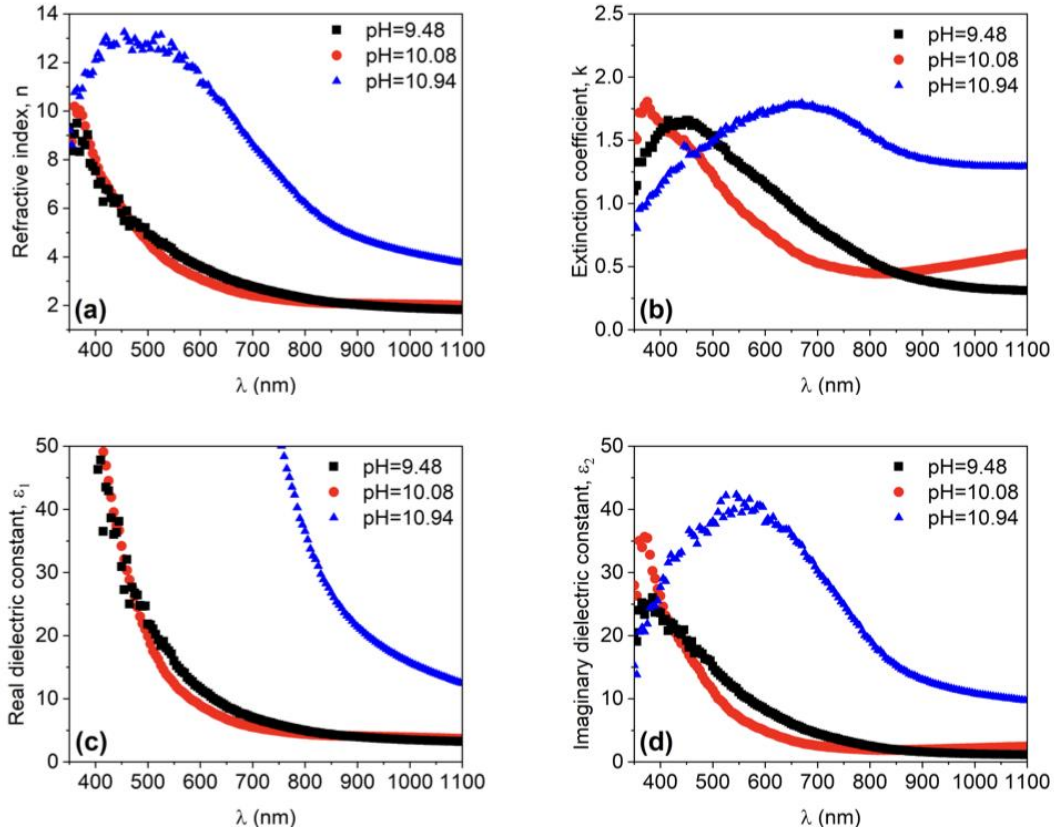

Figure 4. Refractive spectra, (b) extinction spectra, (c) real dielectric constant, and (d) imaginary dielectric constant of the CuO thin films as a function of pH.

Table 2. Film thicknesses and optical parameters of the CuO thin films with varying pH values.

pH	Thickness (nm)	E_g (eV)	λ=600 nm			
			n	k	ε_1	ε_2
9.48	1272	2.18	3.60	1.15	11.63	8.29
10.08	972	2.89	3.10	0.79	8.96	4.89
10.94	1713	1.49	11.14	1.70	121.15	37.90

The real (ε_1) and imaginary (ε_2) parts of complex dielectric constants are defined by the following formulas (Goede et al., 2007):

$$\varepsilon_1 = n^2 + k^2 \tag{10}$$

$$\varepsilon_2 = nk \tag{11}$$

Figure 4(c) and Figure 4(d) indicate the plots of ε_1 and ε_2 with the wavelength. Observed ε_1 and ε_2 values are also illustrated in Table 2. At a 600 nm wavelength, from this table, the ε_1 and ε_2 values for CuO thin films ranged from 8.96 to 121.15 and from 4.89 to 37.90, respectively.

4. Conclusion

In the present work, CuO thin films were produced using a simple, environmental, and low-cost method called the SILAR. The influence of pH on the structural and optical properties of CuO films was systematically investigated. By varying the pH of the bath solution, significant adjustments were observed in the film thickness, crystallite size, direct optical band gap energy, and various optical parameters of the deposited CuO thin films. The highest crystallite size (229.9 nm on $(1\ 1\ \bar{1})$ plane and 252.5 on (2 0 0) plane) and the lowest film thickness (972 nm) were reached for the CuO film produced at pH values of 10.08, respectively. The direct optical band gap energy of the deposited films ranged between 1.49 eV and 2.89 eV. The highest band gap energy was achieved at 2.89 eV for the CuO thin film fabricated at 10.08 pH value.

Notably, films prepared at different pH values exhibited distinct characteristics; for instance, those prepared at pH = 10.08 demonstrated larger crystallite sizes, lower film thicknesses, and higher optical band gap energies compared to films produced at other pH values. Furthermore, comprehensive optical analyses, including parameters such as refractive index (n), extinction coefficient (k), dielectric constants (ε_1) and (ε_2), were conducted to further elucidate the optical behavior of these CuO thin films.

Authors' Contributions

Fatma Göde: Writing-Review & Editing, Writing-Original Draft, Literature Review, Methodology, Performing Experiment, Conceptualization, Formal Analysis. **Ali Çelik:** Writing-Review & Editing, Writing-Original Draft, Literature Review, Methodology, Performing Experiment, Conceptualization.

Statement of Conflicts of Interest

There is no conflict of interest between the authors.

Statement of Research and Publication Ethics

The author declares that this study complies with Research and Publication Ethics.

References

Abdelmoneim, A., K. Elfayoumi, M. A., Sh. Abdel-wahab, M., M. Al-Enizi, A., Key Lee, J., and Tawfik, W.Z. (2024). Enhanced solar-driven photoelectrochemical water splitting using nanoflower Au/CuO/GaN hybrid photoanodes. *RSC Advances*, 14(24), 16846-16858. https://doi.org/10.1039/D4RA01931H

Abeles, F. (1972). *Optical Properties of Solids.* North-Holland, London.

Alami, A. H., Allagui, A., and Alawadhi, H. (2014). Microstructural and optical studies of CuO thin films prepared by chemical ageing of copper substrate in alkaline ammonia solution. *Journal of Alloys and Compounds*, 617, 542-546. https://doi.org/10.1016/j.jallcom.2014.07.221

Anitha, T. V., Gadha Menon, K., Venugopal, K., and Vimalkumar, T. V. (2024). Investigating the role of film thickness on the physical properties of sol-gel coated CuO thin films: Discussing its potentiality in optoelectronic applications. *Materials Science and Engineering: B*, 299, 116960. https://doi.org/10.1016/j.mseb.2023.116960

Arulkumar, E., and Thanikaikarasan, S. (2024). Structure, morphology, composition, optical properties and catalytic activity of nanomaterials CuO, NiO, CuO/NiO using methylene blue. *Optik*, 302, 171685. https://doi.org/10.1016/j.ijleo.2024.171685

Babu, M. H., Podder, J., Dev, B. C., and Sharmin, M. (2020). P to n-type transition with wide blue shift optical band gap of spray synthesized Cd doped CuO thin films for optoelectronic device applications. *Surfaces and Interfaces*, 19, 100459. https://doi.org/10.1016/j.surfin.2020.100459

Chen, Y., Zhang, L., Zhang, H., Zhong, K., Zhao, G., Chen, G., Lin, Y., Chen, S., and Huang, Z. (2018). Band gap manipulation and physical properties of preferred orientation CuO thin films with nano wheatear array. *Ceramics International*, 44(1), 1134-1141. https://doi.org/10.1016/j.ceramint.2017.10.070

Cullity, B. D., and Stock, S. R. (2001). *Elements of X-ray diffraction* (3. ed). Prentice Hall.

Djebian, R., Boudjema, B., Kabir, A., and Sedrati, C. (2020). Physical characterization of CuO thin films obtained by thermal oxidation of vacuum evaporated Cu. *Solid State Sciences*, 101, 106147. https://doi.org/10.1016/j.solidstatesciences.2020.106147

Gnanasekar, T., Valanarasu, S., Poul Raj, I. L., Juliet, A. V., Behera, P. K., Mahmoud, Z. M. M., Shkir, Mohd., and AlFaify, S. (2021). Improved photocurrent properties of La doped CuO thin films coated by nebulizer spray pyrolysis method for photosensor applications. *Optical Materials*, 122, 111790. https://doi.org/10.1016/j.optmat.2021.111790

Gode, F., Guneri, E., and Baglayan, O. (2014). Effect of tri-sodium citrate concentration on structural, optical and electrical properties of chemically deposited tin sulfide films. *Applied Surface Science*, 318, 227-233. https://doi.org/10.1016/j.apsusc.2014.04.128

Goede, C., Guemues, C., and Zor, M. (2007). Influence of the thickness on physical properties of chemical bath deposited hexagonal ZnS thin films. *Journal of Optoelectronıcs and Advanced Materıals*, 9(7). https://avesis.cu.edu.tr/yayin/6da201ec-1689-49cb-b209-a4187af3420e/influence-of-the-thickness-on-physical-properties-of-chemical-bath-deposited-hexagonal-ZnS-thin-films

Göde, F. (2019). Effect of Cu doping on CdS as a multifunctional nanomaterial: Structural, morphological, optical and electrical properties. *Optik*, 197, 163217. https://doi.org/10.1016/j.ijleo.2019.163217

Hassan, J., Karar Mahdi, T., Ghufran Ammar, G., and Qin, C. (2024). Green fabrication of CuO-egTiO2 composite for photodegradation of organic pollutant under direct visible light illumination. *Advanced Powder Technology*, 35(4), 104394. https://doi.org/10.1016/j.apt.2024.104394

Kandulna, R., Rimpi, Das, U., Choudhary, R. B., Kachhap, B., and Kumar, A. (2023). Enriched properties of polypyrrole-copper oxide-reduced graphene oxide (PPY-CuO-rGO) hybrid nanocomposite for organic light emitting diodes (OLEDs) as electron transport layer (ETL) material. *Optik*, 292, 171393. https://doi.org/10.1016/j.ijleo.2023.171393

Kumar, V., Kaphle, A., Rathnasekara, R., Neupane, G. R., and Hari, P. (2024). Role of Al doping in morphology and interface of Al-doped ZnO/CuO film for device performance of thin film-based heterojunction solar cells. *Hybrid Advances*, 5, 100148. https://doi.org/10.1016/j.hybadv.2024.100148

Mageshwari, K., and Sathyamoorthy, R. (2013). Physical properties of nanocrystalline CuO thin films prepared by the SILAR method. *Materials Science in Semiconductor Processing*, 16(2), 337-343. https://doi.org/10.1016/j.mssp.2012.09.016

Narale, D. K., Kumbhar, P. D., Bhosale, R. R., Patil, K. D., Jambhale, C. L., Kim, J. H., and Kolekar, S. S. (2024). Engineering of both binder-free CuCo2O4 nanorod@CuO flower-like nanosheet core-shell heterostructure and NiFe2O4 nanoflake electrodes for asymmetric supercapacitor. *Journal of Energy Storage*, 84, 110942. https://doi.org/10.1016/j.est.2024.110942

Nitta, R., Kubota, Y., Kishi, T., and Matsushita, N. (2022). Fabrication of nanostructured CuO thin films with controllable optical band gaps using a mist spin spray technique at 90 C. *Thin Solid Films*, 762, 139555. https://doi.org/10.1016/j.tsf.2022.139555

Pankove, J. I. (1975). *Optical processes in semiconductors*. Dover Publications, Inc.

Perkowitz, S. (1993). *Optical characterization of semiconductors: Infrared, Raman, and photoluminescence spectroscopy*. Academic Press.

Sagadevan, S., Pal, K., and Chowdhury, Z. Z. (2017). Fabrication of CuO nanoparticles for structural, optical and dielectric analysis using chemical precipitation method. *Journal of Materials Science: Materials in Electronics*, 28(17), 12591-12597. https://doi.org/10.1007/s10854-017-7083-3

Sahu, K., Bisht, A., Khan, S. A., Pandey, A., and Mohapatra, S. (2020). Engineering of morphological, optical, structural, photocatalytic and catalytic properties of nanostructured CuO thin films fabricated by reactive DC magnetron sputtering. *Ceramics International*, 46(6), 7499-7509. https://doi.org/10.1016/j.ceramint.2019.11.248

Shkir, M., Yahia, I. S., Ganesh, V., Algarni, H., and AlFaify, S. (2016). Facile hydrothermal-assisted synthesis of Gd3+ doped PbI2 nanostructures and their characterization. *Materials Letters*, 176, 135-138. https://doi.org/10.1016/j.matlet.2016.04.062

Shkir, M., and AlFaify, S. (2019). A facile low-temperature synthesis of nanosheets assembled PbS microflowers and their structural, morphological, optical, photoluminescence, dielectric and electrical studies. *Material Research. Express*, 6(10), 105013. https://doi.org/10.1088/2053-1591/ab3535

Srinivasan, N. kumar, and Ponnusamy, C. (2024). Influence of various surfactants on the stability and solidification characteristics of DI water-based CuO NFPCM for cool thermal energy storage system. *Journal of Energy Storage*, 86, 111314. https://doi.org/10.1016/j.est.2024.111314

Sultana, J., Paul, S., Karmakar, A., Yi, R., Dalapati, G. K., and Chattopadhyay, S. (2017). Chemical bath deposited (CBD) CuO thin films on n-silicon substrate for electronic and optical applications: Impact of growth time. *Applied Surface Science*, 418, 380-387. https://doi.org/10.1016/j.apsusc.2016.12.139

Yahya Salih, E., Ramizy, A., Sabbar Mohammed, A., Hassan Ibnaouf, K., Hassan Eisa, M., and Aldaghri, O. (2024). Photo-responsive analysis of branchy dendrites-like CuO/PS p-n junction visible light photodetector. *Materials Science and Engineering: B*, 301, 117172. https://doi.org/10.1016/j.mseb.2023.117172

Yousefizad, M., Zarasvand, M. M., Bagheritabar, M., Ghezelayagh, M. M., Farahi, A., Ghafouri, T., Raissi, F., Zeidabadi, M. A., and Manavizadeh, N. (2023). Performance investigation of low-power flexible n-ZnO/p-CuO/n-ZnO heterojunction bipolar transistor: Simulation study. *Micro and Nanostructures*, 180, 207594. https://doi.org/10.1016/j.micrna.2023.207594